Inhibition of the central melanocortin system decreases brown adipose tissue activity[S]

Sander Kooijman,[1,*,†] Mariëtte R. Boon,[*,†] Edwin T. Parlevliet,[*,†,§] Janine J. Geerling,[*,†] Vera van de Pol,[*,†] Johannes A. Romijn,[§] Louis M. Havekes,[*,†,,††] Illiana Meurs,[*,†] and Patrick C. N. Rensen[*,†]**

Department of Endocrinology and Metabolic Diseases,* Einthoven Laboratory for Experimental Vascular Medicine,[†] and Department of Cardiology,** Leiden University Medical Center, Leiden, The Netherlands; Department of Internal Medicine, Academic Medical Center,[§] University of Amsterdam, The Netherlands; and Netherlands Organization for Applied Scientific Research,[††] Gaubius Laboratory, Leiden, The Netherlands

Abstract The melanocortin system is an important regulator of energy balance, and melanocortin 4 receptor (MC4R) deficiency is the most common monogenic cause of obesity. We investigated whether the relationship between melanocortin system activity and energy expenditure (EE) is mediated by brown adipose tissue (BAT) activity. Therefore, female APOE*3-Leiden.CETP transgenic mice were fed a Western-type diet for 4 weeks and infused intracerebroventricularly with the melanocortin 3/4 receptor (MC3/4R) antagonist SHU9119 or vehicle for 2 weeks. SHU9119 increased food intake (+30%) and body fat (+50%) and decreased EE by reduction in fat oxidation (−42%). In addition, SHU9119 impaired the uptake of VLDL-TG by BAT. In line with this, SHU9119 decreased uncoupling protein-1 levels in BAT (−60%) and induced large intracellular lipid droplets, indicative of severely disturbed BAT activity. Finally, SHU9119-treated mice pair-fed to the vehicle-treated group still exhibited these effects, indicating that MC4R inhibition impairs BAT activity independent of food intake. These effects were not specific to the APOE*3-Leiden.CETP background as SHU9119 also inhibited BAT activity in wild-type mice. We conclude that inhibition of central MC3/4R signaling impairs BAT function, which is accompanied by reduced EE, thereby promoting adiposity. We anticipate that activation of MC4R is a promising strategy to combat obesity by increasing BAT activity.— Kooijman, S., M. R. Boon, E. T. Parlevliet, J. J. Geerling, V. van de Pol, J. A. Romijn, L. M. Havekes, I. Meurs, and P. C. N. Rensen. **Inhibition of the central melanocortin system decreases brown adipose tissue activity. *J. Lipid Res.* 2014.** 55: **2022–2032.**

Supplementary key words energy expenditure • liver • triglycerides • very low density lipoprotein • white adipose tissue

The hypothalamus is important in the regulation of energy balance. Activation of pro-opiomelanocortin neurons (e.g., by insulin or leptin) induces secretion of α-melanocyte-stimulating hormone, which in turn stimulates melanocortin 3/4 receptors (MC3/4Rs) within the paraventricular nucleus to cause a negative energy balance (1). Accordingly, activation of central melanocortin 4 receptor (MC4R) in rodent models results in anorexia and weight loss (2), whereas blockade or targeted gene disruption induces hyperphagia and obesity, even on regular chow diet (3, 4). Loss-of-function mutations in MC4R are the most common monogenic form of obesity in humans and are associated with severe obesity in childhood (5). In addition, recent meta-analyses of genome-wide association studies identified common variants near MC4R to influence fat mass, obesity, and obesity risk (6, 7). These observations support an essential role for the melanocortin system in the regulation of energy homeostasis across mammalian species.

In addition to the effects of the melanocortin system on food intake, this system also affects energy balance via other pathways. This notion is supported by the observation that pharmacological inhibition of central MC4R by

This work was supported by 'the Netherlands CardioVascular Research Initiative: the Dutch Heart Foundation, Dutch Federation of University Medical Centers, the Netherlands Organisation for Health Research and Development, and the Royal Netherlands Academy of Sciences' for the GENIUS project 'Generating the best evidence-based pharmaceutical targets for atherosclerosis' (CVON2011-19). P. C. N. Rensen is an Established Investigator of the Netherlands Heart Foundation (Grant 2009T038).

Manuscript received 26 November 2013 and in revised form 27 June 2014.

Published, JLR Papers in Press, July 12, 2014
DOI 10.1194/jlr.M045989

Abbreviations: [^{14}C]CO, [^{14}C]cholesteryl oleate; [^{3}H]TO, glycerol tri[^{3}H]oleate; BAT, brown adipose tissue; CREB, cAMP response element-binding protein; EE, energy expenditure; FFM, fat-free mass; gWAT, gonadal white adipose tissue; iBAT, interscapular brown adipose tissue; MC3/4R, melanocortin 3/4 receptor; MC4R, melanocortin 4 receptor; p-CREB, phosphorylated cAMP response element-binding protein; PL, phospholipid; RER, respiratory exchange ratio; SR-BI, scavenger receptor class B type I; TC, total cholesterol; TH, tyrosine hydroxylase; UCP-1, uncoupling protein-1; WAT, white adipose tissue.

[1] To whom correspondence should be addressed.
e-mail: s.kooijman@lumc.nl

[S] The online version of this article (available at http://www.jlr.org) contains supplementary data in the form of two figures.

icv administration of the synthetic MC3/4R antagonist SHU9119 still increases body fat in pair-fed rats (8). Moreover, the peripheral effects of the central melanocortin system involve alterations in the activity of the sympathetic nervous system (SNS), as icv administration of the MC3/4R agonist MTII dose-dependently increases renal sympathetic activity in mice (9). Furthermore, ablation of neurons that produce agouti-related protein (AgRP), the endogenous antagonist for MC4R, in mice changes autonomic output into metabolic organs, accompanied by a changed respiratory exchange ratio (RER) indicating altered nutrient combustion (10). Additionally, chronic icv SHU9119 treatment in rats increases the RER (8), indicative of reduced lipid utilization. Interestingly, variants near and in the MC4R gene in humans are associated not only with an increased RER (8), but also with reduced total energy expenditure (EE) (11, 12), underscoring the importance of the melanocortin system in the regulation of EE.

A recently discovered and highly important contributor to EE is brown adipose tissue (BAT). BAT contributes to EE by combusting high amounts of TG into heat, a process mediated by uncoupling protein-1 (UCP-1) (13). Interestingly, MC4R-expressing neurons project onto BAT (14), indicating that BAT may mediate the association between MC4R signaling and EE. Therefore, the aim of this study was to evaluate the role of the melanocortin system in BAT activity. For this purpose, we inhibited melanocortin receptor signaling using the MC3/4R antagonist SHU9119 in APOE*3-Leiden.CETP transgenic mice, a well-established model for human-like lipoprotein metabolism.

MATERIALS AND METHODS

Animals and diet

Female APOE*3-Leiden.CETP mice on a C57Bl/6J background (15) were bred at our institutional animal facility and housed under standard conditions with a 12-12 h light-dark cycle with ad libitum access to food and water unless stated otherwise. From 12 to 22 weeks after birth, mice were fed a Western-type diet containing 15% (w/w) cacao butter and 0.1% cholesterol (AB Diets, Woerden, The Netherlands) for the duration of the study to increase plasma levels of apoB-containing lipoproteins, thereby inducing a more human-like lipoprotein profile. After 4 weeks of run-in diet, mice were randomized into groups that received icv administration of artificial cerebrospinal fluid (vehicle) or SHU9119 (5 nmol/day; Bachem, Bubendorf, Germany) in vehicle during 14–17 days. Because SHU9119 induces hyperphagia (3), the effect of SHU9119 on BAT activity independent of food intake was also investigated by using an additional SHU9119-treated group that was pair-fed (SHU9119-pf) to the vehicle-treated group. To achieve pair-feeding, food intake of the ad libitum-fed mice was monitored daily, and pair-fed mice received surgery 1 day behind the control mice. The pair-feeding regimen consisted of giving the mice the average daily consumed food amount by the control mice, just before onset of darkness. To investigate the effect of SHU9119 independent of dyslipidemia induced by Western-type feeding of APOE*3-Leiden.CETP mice, a second experiment was performed using 15-week-old male wild-type C57Bl/6J mice (Charles River) that were housed under similar conditions while being fed a regular chow diet. After 2 weeks of acclimatization, mice were randomized into three groups receiving, for example, vehicle, SHU9119, and SHU9119-pf for 15 days. All animal experiments were approved by the Institutional Ethics Committee on Animal Care and Experimentation at Leiden University Medical Center.

Surgical procedure

For continuous icv administration of SHU9119 versus vehicle, mice were sedated using a mixture of dexmedetomidine (0.5 mg/kg), midazolam (5 mg/kg), and fentanyl (0.05 mg/kg), and cannulas (Brain Infusion Kit 3, ALZET Cupertino, CA) were stereotactically placed in the left lateral ventricle of the brain (coordinates: −0.45 mm anteroposterior, −1.00 mm lateral, and 2.50 mm dorsoventral from bregma). Osmotic minipumps (Model 1004, Alzet, CA) attached to the cannula via a catheter were implanted subcutaneously on the back slightly posterior to the scapulae. The skin was sutured, and the sedation was antagonized with a mixture of antiparnezol (2.5 mg/kg), flumanezil (0.5 mg/kg), and naloxon (1.2 mg/kg). Buprenorphine (0.9 μg) was used as a pain killer. After the surgery, mice were housed individually, and food intake and body weight were monitored on a daily basis. By filling the catheters with vehicle, mice were allowed to recover for 4 days before actually receiving the assigned treatment for 17 days (collection of organs or VLDL production) or 14 days (indirect calorimetry and VLDL clearance).

Body composition

After 17 days of treatment, body composition (lean mass and fat mass) was determined in conscious mice using an EchoMRI-100 (EchoMRI, Houston, TX).

Indirect calorimetry

During the first 5 days of treatment, oxygen uptake ($V\dot{}O_2$), carbon dioxide production ($V\dot{}CO_2$), and physical activity were measured in fully automatic metabolic cages (LabMaster System, TSE Systems, Bad Homburg, Germany). The average RER, EE, carbohydrate, and fat oxidation rates were calculated as described previously (16).

Liver lipid staining and content

Liver samples were perfused with PBS, collected, snap frozen, and stored at −80°C. Sections of 10 μm were cut, fixed in 4% paraformaldehyde, and stained with Oil Red O and Mayer's hematoxylin. Lipids were extracted according to a modified protocol from Bligh and Dyer (17). In short, small liver pieces were homogenized in ice-cold methanol (10 μl/mg tissue); 1.8 ml of $CH_3OH/CHCl_3$ (3:1, v/v) was added to 45 μl of homogenate. After vigorous mixing and centrifugation, the supernatant was dried and suspended in 2% Triton X-100. Concentrations of hepatic TG, total cholesterol (TC), and phospholipids (PLs) were measured using commercially available enzymatic kits for TG (11488872, Roche Diagnostics, Mannheim, Germany), TC (11489232, Roche Diagnostics), and PLs (3009, Instruchemie, Delfzijl, The Netherlands). Liver lipids were expressed per milligram of protein, which was determined using the BCA protein assay kit (Thermo Scientific, Rockford, IL).

VLDL production

After 17 days of treatment, after 4 h of fasting (from 0800 h to 1200 h), the VLDL production rate was assessed. Mice were sedated using a mixture of ventranquil (6.25 mg/kg), dormicum (6.25 mg/kg), and fentanyl (0.31 mg/kg). Subsequently, mice were injected intravenously with 100 μl PBS containing 150 μCi

Tran^{35}S label to measure de novo apoB synthesis, and blood samples were taken via tail bleeding ($t = 0$). Thirty minutes after injection of the Tran^{35}S label, the mice received an iv injection of 500 mg of tyloxapol (Triton WR-1339, Sigma Aldrich, Germany) per kg body weight as 10% (w/w) solution in PBS to block VLDL-TG clearance by LPL-mediated TG hydrolysis. Additional blood samples were taken at $t = 15$, 30, 60, and 90 min after tyloxapol injection and used for determination of plasma TG concentration. After 120 min, the mice were exsanguinated via the retro-orbital plexus. VLDL was isolated from serum after density gradient ultracentrifugation and counted for incorporated ^{35}S-activity. VLDL particle size was determined using a Zetasizer (Malvern Instruments, Malvern, UK), and VLDL lipid composition was determined as described previously.

VLDL clearance experiment

Glycerol tri[^{3}H]oleate ([^{3}H]TO) and [^{14}C]cholesteryl oleate ([^{14}C]CO) double-labeled VLDL-like emulsion particles (80 nm) were prepared as previously described (18). After 14 days of icv SHU9119 or vehicle treatment, mice were fasted for 4 h (from 0800 h to 1200 h) and injected intravenously with the radiolabeled emulsion particles (1.0 mg TG in 200 μl PBS) via the tail vein. At time points $t = 2$, 5, 10, and 15 min after injection, blood was taken from the tail vein to determine the serum decay of both radiolabels. Immediately after the last blood withdrawal, mice were euthanized by cervical dislocation and perfused with ice-cold PBS for 5 min. Organs were harvested and weighed, and the uptake of ^{3}H and ^{14}C radioactivity was determined.

BAT histology

After 17 days of SHU9119 treatment, a part of interscapular BAT (iBAT) was fixed in 4% paraformaldehyde in PBS (pH 7.4) for 24 h, dehydrated, and embedded in paraffin. Sections (10 μm) were cut, rehydrated, and stained with Mayer's hematoxylin and eosin (H&E). To determine sympathetic activation of BAT, a tyrosine hydroxylase (TH) staining was performed. To this end, sections were rehydrated and incubated 15 min with 10 mM citrate buffer (pH 6.0) at 120°C for antigen retrieval. Sections were cooled on ice, washed in PBS and PBS 0.1% Tween, and incubated with 5% BSA/PBS for 60 min at room temperature. This was followed by overnight incubation with 1:2,000 anti-TH (Abcam) primary antibody at 4°C. Next, sections were incubation with secondary antibody (anti-rabbit antibody, DAKO enVision TM) and stained with Nova Red. Nuclei were counterstained with Mayer's hematoxylin, and sections were mounted on glass slides. Percentage of area positive for TH staining was quantified using Image J software.

BAT Western blot analysis

Another part of BAT was snap frozen and stored at −80°C. These BAT samples were homogenized in RIPA buffer and centrifuged, and protein concentration was determined using the BCA protein assay kit (Thermo Scientific). Samples were diluted and denatured for 5 min at 95°C after adding Laemmli Sample Buffer (1:1, v/v; Serva, Heidelberg, Germany). Proteins within homogenates [1 μg protein for UCP-1 and 15 μg for phosphorylated cAMP response element-binding protein (p-CREB)] were separated on a 10% SDS-PAGE gel and subsequently transferred onto blotting membrane. The blotting membranes were then washed with PBS + 0.1% Tween (PBS+T), blocked with 5% milk powder in PBS+T, and incubated overnight at 4°C with the first antibody (anti-UCP-1 rabbit polyclonal; Ab U6382, Sigma Aldrich or anti-p-CREB, Cell Signaling). After washing (PBS+T) the second antibody (anti-rabbit IgG HRP conjugate; 1:5,000; Promega, Madison, WI) was added. After another wash with PBS+T and PBS, SuperSignal Western Blot Enhancer (Thermo Scientific) was added to the blotting membranes, after which they were analyzed with Bio-Rad Quantity One.

BAT gene expression analysis

A part of iBAT from wild-type C57Bl/6J mice treated with vehicle or SHU9119 was snap frozen and stored at −80°C for gene expression analysis and protein analysis (see previous discussion). Total RNA was isolated using TriPure (Roche) according to the manufacturer's instructions. Total RNA (1 μg) was reverse-transcribed using M-MLV reverse transcriptase (Promega). Real-time PCR was carried out on a CFX96 PCR machine (Bio-Rad) using IQ SYBR-Green Supermix (Bio-Rad). Melt curve analysis was included to assure that a single PCR product was formed. Expression levels were normalized using β2-microglobulin as housekeeping gene.

Body temperature

In four wild-type C57Bl/6J mice per group, temperature transponders (IPTT-300, BMDS) were implanted subcutaneously in the clavicular region. Every 3 days, body temperature was recorded using a compatible Smart Probe (BMDS).

Statistical analysis

Differences between groups were determined using independent sample Student's *t*-tests for normally distributed data and Mann-Whitney *U* tests for nonnormal distributed data. Serum decay in the VLDL clearance experiment was analyzed using repeated measurements ANOVA with a Tukey's post hoc test. Probability values <0.05 were considered statistically significant. Data are presented as means ± SEM.

RESULTS

SHU9119 increases body weight and fat mass independent of food intake

APOE*3-Leiden.CETP mice were treated intracerebroventricularly with SHU9119 or vehicle for 17 days. In ad libitum-fed mice, throughout the treatment period, SHU9119 consistently increased food intake (on average 4.04 ± 0.21 vs. 3.18 ± 0.13 g/day, $P < 0.01$) (**Fig. 1A**), concomitantly with an increased body weight gain (after 17 days: 6.68 ± 0.58 vs. 0.70 ± 0.14 g, $P < 0.001$). Obviously, SHU9119 also increased body weight in pair-fed mice when compared with vehicle-treated mice (4.14 ± 0.45 vs. 0.70 ± 0.14 g, $P < 0.01$) (Fig. 1B) indicating that the SHU9119-induced weight gain is independent of food intake. Determination of body composition using EchoMRI revealed that SHU9119 increased body weight under both ad libitum feeding and pair-fed conditions due to a selective increase in fat mass (10.6 ± 1.2 and 9.6 ± 1.0 vs. 4.9 ± 1.1 g, $P < 0.05$) (Fig. 1C). The SHU9119-induced increase in body weight and fat mass was accompanied by an increase in gonadal white adipose tissue (gWAT) weight, both in ad libitum feeding conditions (+124%; 1.32 ± 0.13 vs. 0.59 ± 0.12 g, $P < 0.001$) and pair-fed conditions (+124%; 1.32 ± 0.16 vs. 0.59 ± 0.12 g, $P < 0.01$) (Fig. 1D). SHU9119 increased plasma TG levels in pair-fed mice, while it decreased TC levels in both ad libitum and pair-fed mice (supplementary Fig. I).

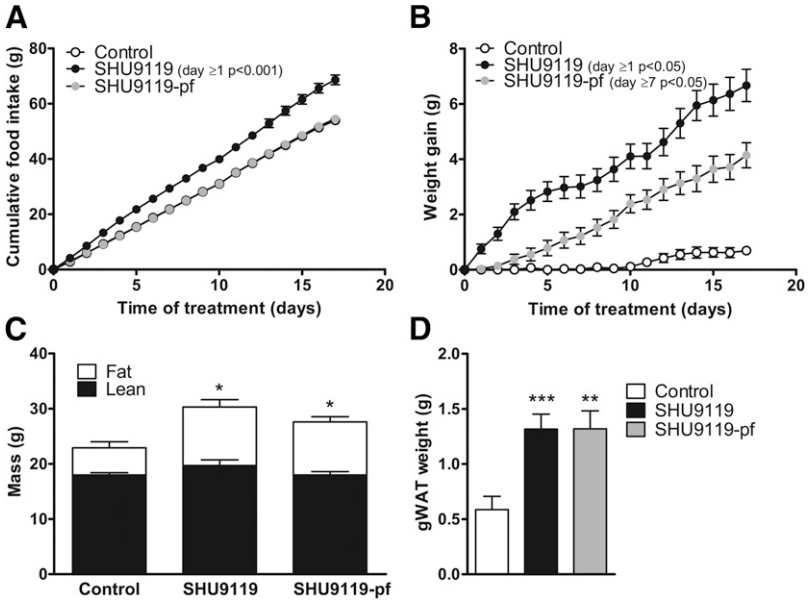

Fig. 1. SHU9119 increases body weight and fat mass independent of food intake. APOE*3-Leiden.CETP mice were treated intracerebroventricularly with vehicle (n = 21) or SHU9119 (5 nmol/day) while being fed ad libitum (n = 21) or being pair-fed (pf) to the vehicle-treated group (n = 22). Food intake (A) and body weight gain (B) were monitored on a daily basis. After 17 days of treatment, lean and fat mass were measured in a random selection of the mice (n = 3–4 per group) using EchoMRI (C). Some of the mice were used for the collection of organs, and weight of gWAT was determined (n = 10–11 per group) (D). Values are means ± SEM. * $P < 0.05$, ** $P < 0.01$, *** $P < 0.001$ compared with control.

In a first experiment, we did observe a large increase in plasma TG levels upon 17 days of SHU9119 treatment under ad libitum conditions (supplementary Fig. IA), which would be consistent with reduced uptake of TG by BAT. However, in a subsequent study, the SHU9119-induced increase in plasma TG only reached significance under pair-fed conditions (supplementary Fig. IB).

SHU9119 reduces whole body fat oxidation independent of food intake

Because SHU9119 induced fat accumulation independent of food intake, we reasoned that SHU9119 likely affected EE. Therefore, we next assessed the effect of SHU9119 on energy metabolism. Fully automated metabolic cages were used during the first 5 days of treatment in order to prevent a potential confounding effect of differences in body weight. Indeed, in ad libitum-fed mice, SHU9119 decreased EE [−10%; 23.7 ± 0.3 vs. 26.4 ± 0.2 cal/h/g fat-free mass (FFM), $P < 0.05$] (**Fig. 2A**) and increased RER (0.92 ± 0.01 vs. 0.88 ± 0.00, $P < 0.01$) (Fig. 2B). These effects were not caused by an effect on carbohydrate oxidation (Fig. 2C) but rather by a large reduction in fat oxidation (−43%; 5.1 ± 1.0 vs. 8.9 ± 0.3 cal/h/g FFM, $P < 0.001$) (Fig. 2D). SHU9119 also reduced activity of the animals (−46%; 67 ± 6 vs. 123 ± 5 A.U., $P < 0.05$; Fig. 2E). Strikingly, the effects of SHU9119 in pair-fed mice, as compared with the control group, were essentially similar as in ad libitum-fed mice with respect to EE (23.9 ± 0.1 cal/h/g FFM, $P < 0.01$), RER (0.91 ± 0.01, $P < 0.01$), fatty acid oxidation (5.3 ± 0.5 cal/h/g FFM, $P < 0.001$), and activity (75 ± 3 A.U., $P < 0.05$). Apparently, SHU9119 reduced EE because of reduced fat oxidation and independent of food intake, as well as a lower locomotor activity.

SHU9119 induces hepatic steatosis due to increased food intake

Because the liver is an important player in TG storage and secretion, we evaluated the effect of SHU9119 on liver weight and TG content as well as on hepatic VLDL-TG secretion. SHU9119 induced hepatomegaly as evidenced by increased liver weight (+85%; 2.17 ± 0.11 vs. 1.17 ± 0.06 g, $P < 0.001$) (**Fig. 3A**) and aggravated hepatic steatosis, as shown by a selective increase in liver TG (+57%; 689 ± 33 vs. 439 ± 37 nmol/mg protein, $P < 0.001$) (Fig. 3B) and neutral lipid staining (Fig. 3C). However, the effects of SHU9119 on the liver were fully attributed to the induction of hyperphagia, as hepatomegaly and hepatic steatosis were not induced under pair-fed conditions (Fig. 3A–C). SHU9119 did not affect the VLDL-TG production rate in mice that were either fed ad libitum (3.39 ± 0.14 mM/h) or pair-fed (3.61 ± 0.37 mM/h) as compared with control mice (3.59 ± 0.29 mM/h) (Fig. 3D, E). The VLDL-apoB production rate was slightly decreased in SHU9119-treated mice, but not in pair-fed SHU9119-treated mice (Fig. 3F). In line with these observations, SHU9119 did not affect VLDL particle size (Fig. 3G), VLDL composition (Fig. 3H), or hepatic expression of the genes *Apob*, *Mttp*, and *Dgat2* involved in VLDL synthesis (not shown). Taken together, SHU9119 induced hepatic steatosis secondary to its induction of hyperphagia and without affecting VLDL-TG secretion.

SHU9119 induces BAT dysfunction independent of food intake

Because BAT strongly contributes to fat oxidation and total EE, we subsequently determined the effect of SHU9119 treatment on BAT function. SHU9119 treatment increased

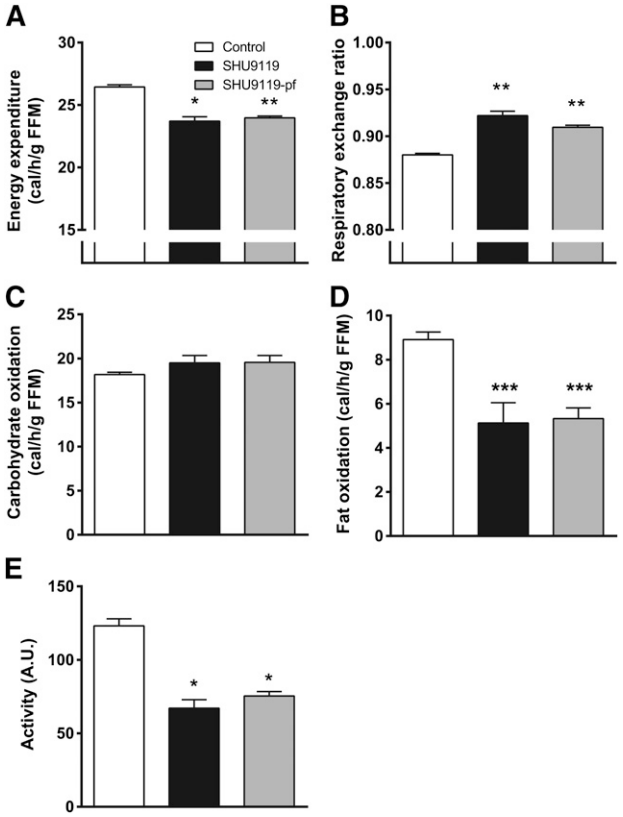

Fig. 2. SHU9119 lowers EE by reducing fat oxidation independent of food intake. APOE*3-Leiden.CETP mice were treated intracerebroventricularly with vehicle (n = 9) or SHU9119 (5 nmol/day) while being fed ad libitum (n = 6) or being pair-fed (pf) to the vehicle-treated group (n = 9). During the first 5 days of treatment, mice were housed in fully automated metabolic cages. EE (A), RER (B), carbohydrate oxidation (C), and fat oxidation (D) were calculated from O_2 uptake and CO_2 excretion. Locomotor activity (E) was measured by infrared-light beam breaks. Values are means ± SEM. * $P < 0.05$, ** $P < 0.01$, *** $P < 0.001$ compared with control.

BAT weight in ad libitum-fed mice (+50%; 0.15 ± 0.01 vs. 0.10 ± 0.01 g, $P < 0.01$) and tended to increase BAT weight in pair-fed animals (+24%; 0.13 ± 0.01 g, $P = 0.06$) (**Fig. 4A**). Strikingly, SHU9119 dramatically increased intracellular lipid droplet size in BAT in both ad libitum-fed and pair-fed mice (Fig. 4B), along with reduced sympathetic innervation of BAT as evidenced by reduced TH (i.e., the rate-limiting enzyme in noradrenaline synthesis) (−53%, $P < 0.001$ and −43%, $P < 0.001$) (Fig. 4C–D) and reduced phosphorylation of CREB (−22%, $P < 0.05$ and −15%, nonsignificant) (Fig. 4E), a downstream target of β3-adrenergic signaling. Accordingly, largely reduced UCP-1 protein levels in BAT (−61%, $P < 0.001$ and −61%, $P < 0.001$) were observed (Fig. 4F). These data imply that SHU9119 decreases BAT activity independent of food intake, likely due to lower sympathetic innervation of BAT, and this may result in decreased burning of intracellulary stored TG and, as a consequence, larger intracellular lipid droplet size.

To assess the capacity of BAT to take up VLDL-TG, we next determined the effect of SHU9119 on the kinetics of iv injected [^{3}H]TO and [^{14}C]CO double-labeled VLDL-like emulsion particles after 14 days of treatment. SHU9119 impaired the plasma decay of [^{3}H]TO (Fig. 4G) and [^{14}C]CO (Fig. 4I) under ad libitum-fed conditions, and that of [^{14}C]CO under pair-fed conditions (Fig. 4I). At 15 min after injection, the distribution of radiolabels over the organs was assessed. In control mice, the uptake of [^{3}H]TO-derived activity by BAT (31.6 ± 8.0%/g) was much higher than the uptake by liver (∼4-fold), muscle (∼25-fold), and WAT (∼25-fold), indicating that BAT is highly metabolically active compared with other organs. Interestingly, SHU9119 tended to selectively decrease the uptake of [^{3}H]TO by BAT in the ad libitum-fed group and significantly did so in mice pair-fed to the control group (−57%; 13.7 ± 1.9% of injected dose/g, $P < 0.05$) (Fig. 4H), most likely as a consequence of reduced hydrolysis of VLDL-TG. Indeed, in the control group, as compared with the ^{3}H-label, the uptake of the ^{14}C-label was much lower in BAT (∼10-fold), muscle (∼4-fold), heart (∼3-fold), and WAT (∼3-fold), while the uptake of ^{14}C-label was higher in liver (∼3-fold). This pattern is compatible with selective delipidation of the VLDL-like emulsion particles in plasma by the LPL-expressing tissues (i.e., uptake of ^{3}H activity), with subsequent uptake of the core remnant by the liver (i.e., uptake of ^{14}C activity). SHU9119 treatment tended to reduce the uptake of [^{14}C]CO in the liver of both ad libitum-fed mice (−20%; 20.8 ± 3.6%/g, $P = 0.11$) and pair-fed mice (−11%; 23.1 ± 1.5%/g, $P = 0.25$) as compared with the control group (26.1 ± 2.1%/g), whereas it decreased the uptake of [^{14}C]CO by BAT (ad libitum-fed mice: −39%, $P = 0.24$; pair-fed mice: −57%, $P < 0.01$) (Fig. 4J).

SHU9119 also induces BAT dysfunction independent of dyslipidemia

To investigate the inhibitory effects of SHU9119 on BAT activity independent of dyslipidemia induced by Western-type diet feeding in APOE*3-Leiden.CETP mice, we next repeated experiments in wild-type mice that were fed a regular chow diet. Again, SHU9119 consistently increased food intake (on average 4.97 ± 0.29 vs. 4.10 ± 0.26 g/day, $P < 0.05$) (**Fig. 5A**) accompanied by an increase in body weight gain (5.43 ± 0.58 vs. 0.21 ± 0.24 g, $P < 0.001$) (Fig. 5B). As with the APOE*3-Leiden.CETP mice, administration of SHU9119 in wild-type mice increased body weight gain in pair-fed animals (1.29 ± 0.32 g, $P < 0.05$) (Fig. 5B), due to a selective increase in fat mass (Fig. 5C). Histological analysis revealed increased lipid accumulation in BAT upon SHU9119 treatment (Fig. 5D), especially in the ad libitum-fed mice in which 51 ± 14% of the total area consisted of lipids ($P < 0.001$) (Fig. 5E). In addition, SHU9119 tended to reduce TH content in BAT in both ad libitum and pair-fed mice (−32% and −42%, respectively) (Fig. 5F), accompanied by reduced phosphorylation of CREB (−32%, $P < 0.01$ and −52%, $P < 0.001$, respectively) (Fig. 5G), supporting reduced sympathethic innervation of BAT. Again, SHU9119 markedly reduced UCP-1 protein content in BAT in both ad libitum and pair-fed mice (−54%, $P < 0.001$ and −64%, $P < 0.001$, respectively) (Fig. 5H). SHU9119 resulted in lower body temperature in both ad libitum (35.9 ± 0.32°C, $P < 0.01$)

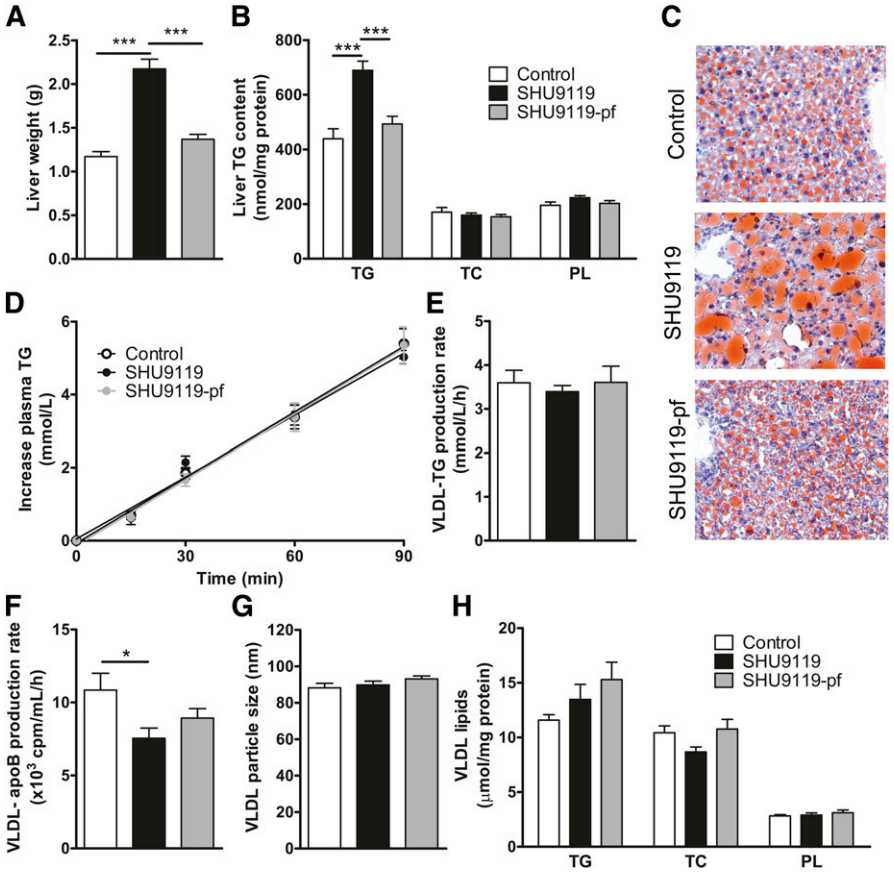

Fig. 3. SHU9119 induces hepatomegaly and steatosis only in ad libitum-fed mice. APOE*3-Leiden.CETP mice were treated intracerebroventricularly with vehicle (n = 21) or SHU9119 (5 nmol/day) while being fed ad libitum (n = 21) or being pair-fed (pf) to the vehicle-treated group (n = 20). After 17 days of treatment, some of the mice were euthanized (n = 10–11 per group) to collect organs and determine liver weight (A), and to determine liver content of TGs, TC, and PLs (B). Frozen liver samples were sectioned and stained with a neutral lipid staining (Oil Red O) and hematoxylin, and representative pictures are shown (C). The remaining mice (n = 8–10 per group) were fasted 4 h, and consecutively injected with Tran^{35}S label and tyloxapol, and blood samples were drawn up to 90 min after tyloxapol injection. Plasma TG concentration was determined and plotted as the increase in plasma TG relative to $t = 0$ (D). The rate of TG production was calculated from the slopes of the curves from the individual mice (E). After 120 min, the total VLDL fraction was isolated by ultracentrifugation, and the rate of newly synthesized VLDL-apoB was determined (F). The VLDL fractions were assayed for particle size (G) and lipid content (H). Values are means ± SEM. * $P < 0.05$, *** $P < 0.001$ compared with control.

and pair-fed (35.6 ± 0.47°C, $P < 0.05$) animals as compared with vehicle-treated mice (36.7 ± 0.46°C) (Fig. 5I, J), which is in line with reduced BAT thermogenesis. We next assessed the capacity of BAT to take up VLDL-TG upon SHU9119 treatment. Again, SHU9119 lowered uptake of [^{3}H]TO-derived activity from VLDL-like emulsion particles by BAT in ad libitum-fed mice compared with vehicle-treated animals (−80%, $P < 0.001$). Interestingly, in pair-fed animals this effect was not observed (Fig. 5K). Accordingly, gene expression of the lipolytic enzyme *Lpl* was decreased in ad libitum-fed mice (−70%, $P < 0.001$), but not in pair-fed mice (Fig. 5L). These data suggest that lower local hydrolysis of TG-rich lipoprotein-like particles may well underlie the lower uptake of TG by BAT upon SHU9119 treatment. Altogether, SHU9119 inhibits BAT activity in both hyperlipidemic APOE*3-Leiden.CETP mice and normolipidemic wild-type mice.

DISCUSSION

The melanocortin system is an important regulator of energy balance, and MC4R deficiency is the most common monogenic cause of obesity. BAT recently emerged as an important player in EE by combusting high amounts of TG toward heat. In addition, MC4R-expressing neurons project onto BAT (14). Hence, the association between MC4R and EE may be mediated by BAT. In the current study, we aimed to evaluate the direct effect of the melanocortin system on BAT activity. For this purpose, we inhibited the central melanocortin system using the MC3/4R synthetic antagonist SHU9119 in APOE*3-Leiden.CETP mice. We found that icv administration of SHU9119 decreased EE and BAT activity, concomitant with selectively impaired uptake of TG from plasma by BAT, independent of food intake.

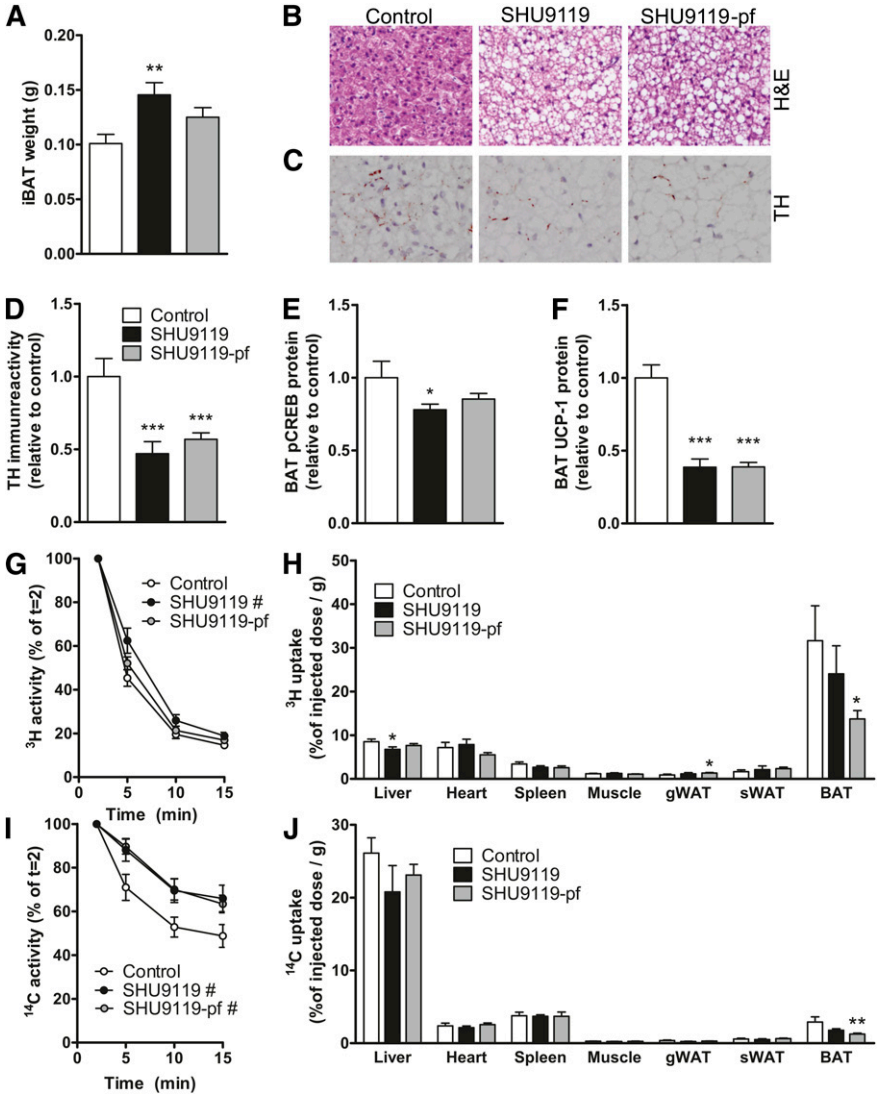

Fig. 4. SHU9119 causes malfunction of BAT. APOE*3-Leiden.CETP mice were treated intracerebroventricularly with vehicle (n = 21) or SHU9119 (5 nmol/day) while being fed ad libitum (n = 21) or being pair-fed (pf) to the vehicle-treated group (n = 22). After 17 days of treatment, some of the mice were euthanized (n = 10–11 per group), and iBAT was quantitatively removed. iBAT was examined for weight (A), morphology, as assessed by H&E staining (B), and TH content (C, D). In iBAT, protein content of p-CREB (E) and UCP-1 (F) were determined. In a second experiment, after 14 days of icv treatment with vehicle (n = 8) or SHU9119 (5 nmol/day) while being fed ad libitum (n = 5) or being pf to the vehicle-treated group (n = 9), mice were fasted 4 h and consecutively injected with [^{3}H]TO- and [^{14}C]CO-labeled VLDL-like emulsion particles. Plasma [^{3}H]TO (G) and [^{14}C]CO (H) were determined at the indicated time points and plotted relative to the dosage at $t = 2$ min. At 15 min after injection, organs were isolated, and uptake of the ^{3}H-activity (H) and ^{14}C-activity (J) was determined. Values are means ± SEM. $^{\#}$ $P < 0.05$, * $P < 0.05$, ** $P < 0.01$, *** $P < 0.001$ compared with control.

Both in ad libitum as well in pair-fed conditions, SHU9119 treatment increased body weight and WAT mass. These data are in line with those of Nogueiras et al. (8), who attributed weight gain and adiposity upon SHU9119 treatment to an increase in both lipid uptake as well as TG synthesis for storage in WAT. Accordingly, we found enhanced uptake of TG by gWAT after a bolus injection of double-labeled VLDL-like emulsion particles. Though the increase in TG uptake by gWAT may have seemed small when expressed per gram of tissue, the total depot of gWAT may contribute to a marked absolute TG uptake by the tissue. We also showed that in ad libitum-fed conditions, SHU9119 induced ectopic lipid deposition in the liver, manifested by hepatomegaly and hepatic steatosis. Hepatic steatosis did not develop in pair-fed mice, indicating that this effect is a direct consequence of SHU9119-induced hyperphagia. Similar effects on the liver are observed after 4 days of icv SHU9119 treatment in rats (19) and in MC4R-deficient mice, which in addition develop steatohepatitis when fed a high-fat diet and have therefore been proposed as a novel mouse model for non-alcoholic steatohepatitis (20). Although hepatic steatosis

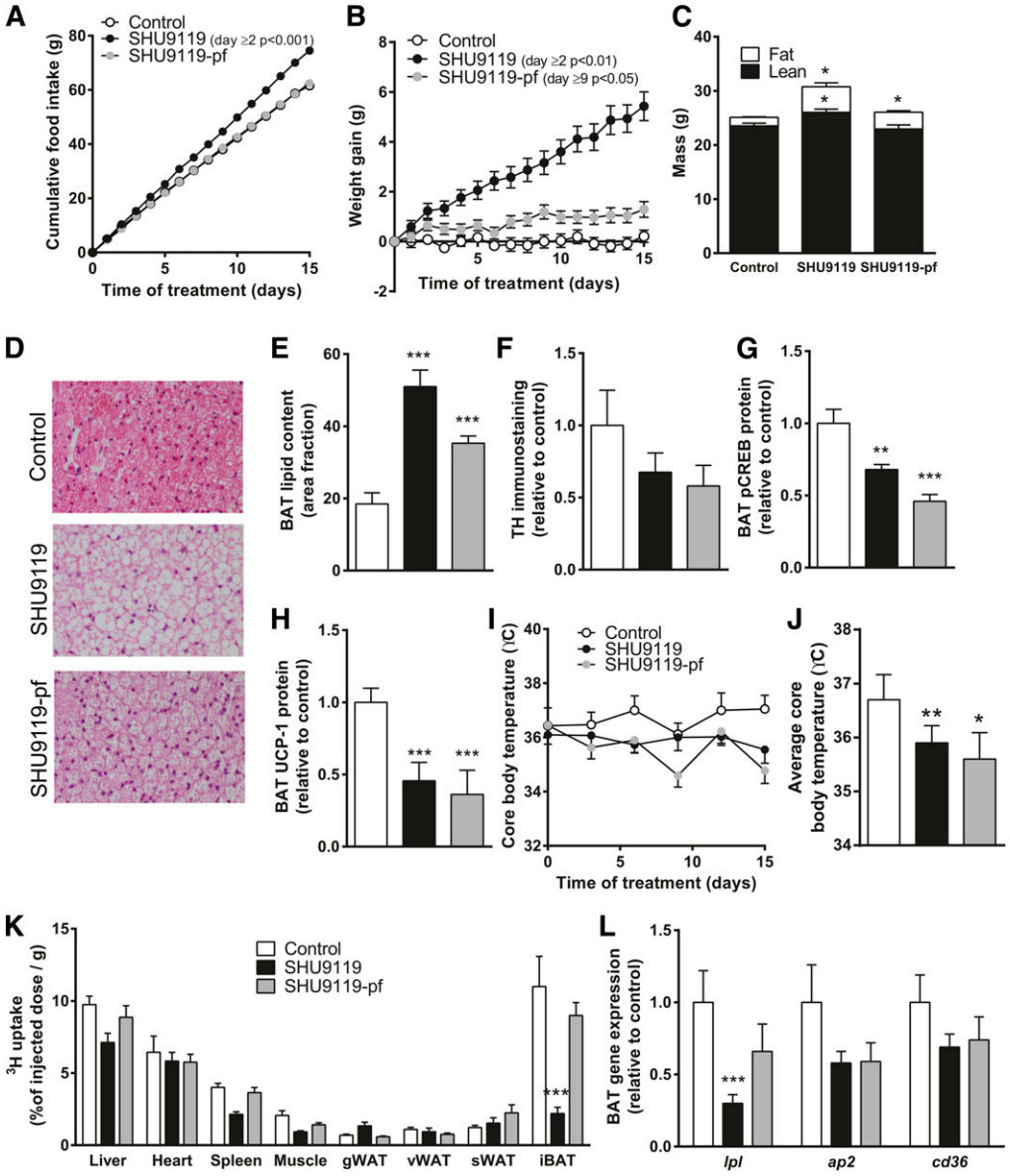

Fig. 5. SHU9119 induces BAT dysfunction independent of dyslipidemia. Wild-type C57Bl/6J mice were treated intracerebroventricularly with vehicle (n = 9) or SHU9119 (5 nmol/day) while being fed ad libitum (n = 10) or being pair-fed (pf) to the vehicle-treated group (n = 9). Food intake (A) and body weight (B) were monitored on a daily basis. After 15 days, body composition was determined using EchoMRI (C). On a histological level, morphology was assessed by H&E staining (D), lipid content was quantified (E), and TH immunoreactivity was determined (F). BAT protein levels of p-CREB (G) and UCP-1 (H) were measured using Western blots. Core body temperature was measured every 3 days using subcutaneously implanted temperature transponder (I) and average core body temperature was calculated (J). Before scarification, after 4 h of fasting, mice were injected with [^{3}H]TO-labeled VLDL-like emulsion particles and organs were isolated 15 min after injection. Uptake of the ^{3}H-activity (K) was determined and frozen sections were used to determine gene expression (L). Values are means ± SEM. * $P < 0.05$, ** $P < 0.05$, *** $P < 0.001$ compared with control.

could promote the secretion of hepatic lipid as VLDL (21), SHU9119 did not increase the VLDL-TG production, VLDL-size, or composition of newly synthesized VLDL. Our data corroborate those of Stafford et al. (22) who showed that a single icv injection of 15 μg SHU9119 does not affect VLDL-TG production in rats. Of note, apoB production was decreased in ad libitum-fed SHU9119-treated animals, which may be the consequence of the hepatic steatosis. These data corroborate previous observations that steatosis, by inducing ER stress, inhibits the hepatic production of apoB100 (23), which can result in production of large lipid-rich VLDL particles (24).

Because SHU9119 was able to increase body adiposity independent of a change in food intake, we reasoned that SHU9119 reduced EE. Indeed, by performing studies with metabolic cages, we confirmed that inhibition of the central melanocortin system reduced EE. Besides decreasing locomotor activity, SHU9119 selectively reduced fat

oxidation, whereas carbohydrate oxidation remained unaffected. This reduction in fat oxidation and total EE occurred independently of food intake and before changes in body weight were observed, indicative of a causal relation between reduced EE and the induction of obesity. Likewise, a previous study has shown that 7 days of icv injections with SHU9119 in rats increased the RER and thereby decreased fat utilization independent of food intake (8). As locomotor activity was not affected in that study, reduced fat oxidation may be dominant over the effect of decreased locomotor activity in the decrease in EE. In addition, MC4R-deficient humans also display an increase in RER (8). Taken together, we suggest that, in general, inhibition of the melanocortin system results in a shift toward decreased metabolic use of lipids leading to elevated fat deposition in WAT.

Because BAT is a highly active metabolic tissue involved in EE and regulation of weight gain, we next proposed that the reduction in fat oxidation could be largely attributed to decreased activity of BAT. Indeed, in both ad libitum and pair-fed conditions in APOE*3-Leiden.CETP mice fed a Western-type diet, analysis of BAT revealed that SHU9119 largely increased intracellular lipid stores and decreased the protein level of the UCP-1, both indicative of reduced BAT activity (25). These data corroborate previous findings showing that chronic icv treatment of ad libitum-fed rats with SHU9119 lowered BAT temperature during the night (26). Moreover, seven daily icv injections of AgRP, the endogenous antagonist for MC4R, decreased *Ucp1* gene expression in pair-fed rats (27), while acute icv injections of glucagon-like peptide-1, which indirectly stimulates MC4R, increased BAT thermogenesis by increasing activity of the sympathetic fibers toward BAT (28). Accordingly, because the activity of BAT is dependent on SNS outflow from the hypothalamus (29, 30), reduced sympathetic output from the hypothalamus toward BAT is the likely mechanism by which inhibition of the central melanocortin system reduced BAT activity. We observed reduced sympathetic output toward BAT as evidenced by decreased levels of TH, the rate-limiting enzyme in noradrenalin synthesis, and decreased phosphorylation of CREB, a downstream target of β3-adrenergic signaling, in BAT upon SHU9119 treatment. Thus, these data support a major role for BAT in the reduced EE and enhanced weight gain of central MC4R inhibition. However, based on these data, we cannot exclude the involvement of other metabolic tissues such as liver and WAT in the development of the disadvantageous metabolic phenotype.

Interestingly, in the APOE*3-Leiden.CETP mice fed a Western-type diet, we provided evidence that SHU9119 lowered both β-oxidation and VLDL-TG uptake by BAT, while lipid accumulation was markedly enhanced. This suggests that the lower β-oxidation upon SHU9119 treatment was more pronounced than the reduced VLDL-TG uptake by the tissue. It would make physiological sense if the reduction in VLDL-TG uptake by BAT occurred as a secondary mechanism to compensate for the diminished TG combustion by the tissue. Indeed, this is supported by the study performed in chow-fed wild-type C57Bl/6J mice. While both the ad libitum-fed and pair-fed animals developed marked lipid accumulation in BAT upon SHU9119 treatment, only the ad libitum-fed mice exhibited lower TG uptake by BAT. Of note, the lipid accumulation in BAT was less pronounced in the C57Bl6/J mice pair-fed chow as compared with the APOE*3-Leiden.CETP mice pair-fed a Western-type diet, perhaps due to the lower fat content of the chow diet. It is, therefore, likely that especially brown adipocytes that become saturated with lipids lower their TG uptake as a secondary mechanism, for instance by downregulation of *Lpl* expression resulting in lower VLDL-TG hydrolysis. Indeed, in the study with C57Bl6/J mice, *Lpl* was downregulated only in the SHU9119 mice that were fed ad libitum.

Recently, Bartelt et al. (13) identified BAT as a major organ involved in plasma VLDL-TG clearance, with 24 h of cold induction resulting in normalization of plasma TG

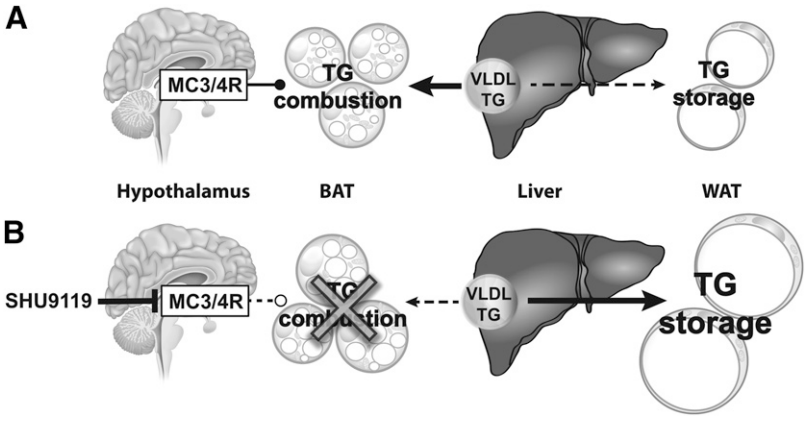

Fig. 6. Proposed model of the effect of SHU9119 on peripheral TG metabolism. Under physiological conditions, MC3/4R signaling is required for basal combustion of VLDL-derived TGs in BAT, preventing storage of excess TG in WAT (A). Inhibition of central MC3/4R signaling by SHU9119 reduces BAT activity, thereby reducing the uptake and combustion of VLDL-TG by BAT. As a consequence, excess TG is stored in WAT, independent of SHU9119-induced hyperphagia (B).

levels in hypertriglyceridemic mice. To investigate the effects of decreased BAT activity on plasma lipid levels, dyslipidemic APOE*3-Leiden.CETP mice were used in the first set of experiments. In a first experiment, we did observe a large increase in plasma TG levels upon 17 days of SHU9119 treatment under ad libitum conditions (supplementary Fig. IA), which would be consistent with reduced uptake of TG by BAT. However, in a subsequent study, the SHU9119-induced increase in plasma TG only reached significance under pair-fed conditions (supplementary Fig. IB). Likewise, icv infusion of the MC4R synthetic antagonist HS104 also failed to increase plasma TG levels in pair-fed rats (31). It should be noted that MC4R-deficient mice have only modestly increased plasma TG levels compared with control mice (+30%) (32), implying that partial inhibition of MC4R by SHU9119 may be insufficient to significantly increase plasma TG levels. In heterozygous MC4R-deficient subjects, plasma TG levels are increased (1.7 vs. 1.3 mM) (33), indicating that the melanocortin system does play a role in the regulation of plasma VLDL-TG levels in humans.

Recently, Perez-Tilve et al. (34) demonstrated that inhibition of the central melanocortin neurons by either ghrelin or SHU9119 in wild-type mice increased circulating cholesterol, related to a decreased hepatic expression of scavenger receptor class B type I (SR-BI) involved in the selective hepatic uptake of HDL-cholesteryl esters. In our study in APOE*3-Leiden.CETP mice with a human-like lipoprotein metabolism, SHU9119 did not decrease TC levels (supplementary Fig. I) despite decreased hepatic SR-BI expression (supplementary Fig. II). This is likely due to the expression of human cholesteryl ester transfer protein (CETP) that provides an alternative route for the clearance of HDL-cholesterol, as CETP expression in SR-BI-deficient mice also precludes an increase in HDL-cholesterol (35). In addition, this could be related to an increased output of cholesterol in the feces as well as a somewhat reduced output of cholesterol from the liver within VLDL. Likewise, humans with heterozygous MC4R deficiency also do not have increased cholesterol levels (33), pointing to a species-dependent effect of MC4R function on HDL-cholesterol levels.

In conclusion, inhibition of central MC3/4R signaling by SHU9119 reduces BAT activity, thereby reducing the uptake and combustion of VLDL-TG by BAT. As a consequence, excess lipids are stored in WAT (**Fig. 6**). We anticipate that MC4R agonists that are currently in development to combat obesity increase EE through activation of BAT.

REFERENCES

1. Garfield, A. S., D. D. Lam, O. J. Marston, M. J. Przydzial, and L. K. Heisler. 2009. Role of central melanocortin pathways in energy homeostasis. *Trends Endocrinol. Metab.* **20:** 203–215.
2. Nargund, R. P., A. M. Strack, and T. M. Fong. 2006. Melanocortin-4 receptor (MC4R) agonists for the treatment of obesity. *J. Med. Chem.* **49:** 4035–4043.
3. Fan, W., B. A. Boston, R. A. Kesterson, V. J. Hruby, and R. D. Cone. 1997. Role of melanocortinergic neurons in feeding and the agouti obesity syndrome. *Nature.* **385:** 165–168.
4. Huszar, D., C. A. Lynch, V. Fairchild-Huntress, J. H. Dunmore, Q. Fang, L. R. Berkemeier, W. Gu, R. A. Kesterson, B. A. Boston, R. D. Cone, et al. 1997. Targeted disruption of the melanocortin-4 receptor results in obesity in mice. *Cell.* **88:** 131–141.
5. Farooqi, I. S., J. M. Keogh, G. S. Yeo, E. J. Lank, T. Cheetham, and S. O'Rahilly. 2003. Clinical spectrum of obesity and mutations in the melanocortin 4 receptor gene. *N. Engl. J. Med.* **348:** 1085–1095.
6. Loos, R. J., C. M. Lindgren, S. Li, E. Wheeler, J. H. Zhao, I. Prokopenko, M. Inouye, R. M. Freathy, A. P. Attwood, J. S. Beckmann, et al. 2008. Common variants near MC4R are associated with fat mass, weight and risk of obesity. *Nat. Genet.* **40:** 768–775.
7. Xi, B., G. R. Chandak, Y. Shen, Q. Wang, and D. Zhou. 2012. Association between common polymorphism near the MC4R gene and obesity risk: a systematic review and meta-analysis. *PLoS ONE.* **7:** e45731.
8. Nogueiras, R., P. Wiedmer, D. Perez-Tilve, C. Veyrat-Durebex, J. M. Keogh, G. M. Sutton, P. T. Pfluger, T. R. Castaneda, S. Neschen, S. M. Hofmann, et al. 2007. The central melanocortin system directly controls peripheral lipid metabolism. *J. Clin. Invest.* **117:** 3475–3488.
9. Rahmouni, K., W. G. Haynes, D. A. Morgan, and A. L. Mark. 2003. Role of melanocortin-4 receptors in mediating renal sympathoactivation to leptin and insulin. *J. Neurosci.* **23:** 5998–6004.
10. Joly-Amado, A., R. G. Denis, J. Castel, A. Lacombe, C. Cansell, C. Rouch, N. Kassis, J. Dairou, P. D. Cani, R. Ventura-Clapier, et al. 2012. Hypothalamic AgRP-neurons control peripheral substrate utilization and nutrient partitioning. *EMBO J.* **31:** 4276–4288.
11. Cole, S. A., N. F. Butte, V. S. Voruganti, G. Cai, K. Haack, J. W. Kent, Jr., J. Blangero, A. G. Comuzzie, J. D. McPherson, and R. A. Gibbs. 2010. Evidence that multiple genetic variants of MC4R play a functional role in the regulation of energy expenditure and appetite in Hispanic children. *Am. J. Clin. Nutr.* **91:** 191–199.
12. Krakoff, J., L. Ma, S. Kobes, W. C. Knowler, R. L. Hanson, C. Bogardus, and L. J. Baier. 2008. Lower metabolic rate in individuals heterozygous for either a frameshift or a functional missense MC4R variant. *Diabetes.* **57:** 3267–3272.
13. Bartelt, A., O. T. Bruns, R. Reimer, H. Hohenberg, H. Ittrich, K. Peldschus, M. G. Kaul, U. I. Tromsdorf, H. Weller, C. Waurisch, et al. 2011. Brown adipose tissue activity controls triglyceride clearance. *Nat. Med.* **17:** 200–205.
14. Voss-Andreae, A., J. G. Murphy, K. L. Ellacott, R. C. Stuart, E. A. Nillni, R. D. Cone, and W. Fan. 2007. Role of the central melanocortin circuitry in adaptive thermogenesis of brown adipose tissue. *Endocrinology.* **148:** 1550–1560.
15. Westerterp, M., C. C. van der Hoogt, W. de Haan, E. H. Offerman, G. M. Dallinga-Thie, J. W. Jukema, L. M. Havekes, and P. C. Rensen. 2006. Cholesteryl ester transfer protein decreases high-density lipoprotein and severely aggravates atherosclerosis in APOE*3-Leiden mice. *Arterioscler. Thromb. Vasc. Biol.* **26:** 2552–2559.
16. Van Klinken, J. B., S. A. van den Berg, L. M. Havekes, and K. Willems van Dijk. 2012. Estimation of activity related energy expenditure and resting metabolic rate in freely moving mice from indirect calorimetry data. *PLoS ONE.* **7:** e36162.
17. Bligh, E. G., and W. J. Dyer. 1959. A rapid method of total lipid extraction and purification. *Can. J. Biochem. Physiol.* **37:** 911–917.
18. Rensen, P. C., N. Herijgers, M. H. Netscher, S. C. Meskers, M. van Eck, and T. J. Van Berkel. 1997. Particle size determines the specificity of apolipoprotein E-containing triglyceride-rich emulsions for the LDL receptor versus hepatic remnant receptor in vivo. *J. Lipid Res.* **38:** 1070–1084.
19. Wiedmer, P., N. Chaudhary, M. Rath, C. X. Yi, G. Ananthakrishnan, R. Nogueiras, E. K. Wirth, H. Kirchner, U. Schweizer, W. Jonas, et al. 2012. The HPA axis modulates the CNS melanocortin control of liver triacylglyceride metabolism. *Physiol. Behav.* **105:** 791–799.
20. Itoh, M., T. Suganami, N. Nakagawa, M. Tanaka, Y. Yamamoto, Y. Kamei, S. Terai, I. Sakaida, and Y. Ogawa. 2011. Melanocortin 4 receptor-deficient mice as a novel mouse model of nonalcoholic steatohepatitis. *Am. J. Pathol.* **179:** 2454–2463.
21. Adiels, M., M. R. Taskinen, C. Packard, M. J. Caslake, A. Soro-Paavonen, J. Westerbacka, S. Vehkavaara, A. Hakkinen, S. O. Olofsson, H. Yki-Jarvinen, et al. 2006. Overproduction of large VLDL particles is driven by increased liver fat content in man. *Diabetologia.* **49:** 755–765.
22. Stafford, J. M., F. Yu, R. Printz, A. H. Hasty, L. L. Swift, and K. D. Niswender. 2008. Central nervous system neuropeptide Y signaling modulates VLDL triglyceride secretion. *Diabetes.* **57:** 1482–1490.
23. Ota, T., C. Gayet, and H. N. Ginsberg. 2008. Inhibition of apolipoprotein B100 secretion by lipid-induced hepatic endoplasmic reticulum stress in rodents. *J. Clin. Invest.* **118:** 316–332.

24. Werner, A., R. Havinga, T. Bos, V. W. Bloks, F. Kuipers, and H. J. Verkade. 2005. Essential fatty acid deficiency in mice is associated with hepatic steatosis and secretion of large VLDL particles. *Am. J. Physiol. Gastrointest. Liver Physiol.* **288:** G1150–G1158.
25. Carobbio, S., B. Rosen, and A. Vidal-Puig. 2013. Adipogenesis: new insights into brown adipose tissue differentiation. *J. Mol. Endocrinol.* **51:** T75–T85.
26. Verty, A. N., A. M. Allen, and B. J. Oldfield. 2010. The endogenous actions of hypothalamic peptides on brown adipose tissue thermogenesis in the rat. *Endocrinology.* **151:** 4236–4246.
27. Small, C. J., M. S. Kim, S. A. Stanley, J. R. Mitchell, K. Murphy, D. G. Morgan, M. A. Ghatei, and S. R. Bloom. 2001. Effects of chronic central nervous system administration of agouti-related protein in pair-fed animals. *Diabetes.* **50:** 248–254.
28. Lockie, S. H., K. M. Heppner, N. Chaudhary, J. R. Chabenne, D. A. Morgan, C. Veyrat-Durebex, G. Ananthakrishnan, F. Rohner-Jeanrenaud, D. J. Drucker, R. DiMarchi, et al. 2012. Direct control of brown adipose tissue thermogenesis by central nervous system glucagon-like peptide-1 receptor signaling. *Diabetes.* **61:** 2753–2762.
29. Bartness, T. J., C. H. Vaughan, and C. K. Song. 2010. Sympathetic and sensory innervation of brown adipose tissue. *Int. J. Obes. (Lond).* **34 (Suppl. 1):** S36–S42.
30. Morrison, S. F., C. J. Madden, and D. Tupone. 2012. Central control of brown adipose tissue thermogenesis. *Front. Endocrinol. (Lausanne).* **3:** 5.
31. Baran, K., E. Preston, D. Wilks, G. J. Cooney, E. W. Kraegen, and A. Sainsbury. 2002. Chronic central melanocortin-4 receptor antagonism and central neuropeptide-Y infusion in rats produce increased adiposity by divergent pathways. *Diabetes.* **51:** 152–158.
32. Iqbal, J., X. Li, B. H. Chang, L. Chan, G. J. Schwartz, S. C. Chua, Jr., and M. M. Hussain. 2010. An intrinsic gut leptin-melanocortin pathway modulates intestinal microsomal triglyceride transfer protein and lipid absorption. *J. Lipid Res.* **51:** 1929–1942.
33. Greenfield, J. R., J. W. Miller, J. M. Keogh, E. Henning, J. H. Satterwhite, G. S. Cameron, B. Astruc, J. P. Mayer, S. Brage, T. C. See, et al. 2009. Modulation of blood pressure by central melanocortinergic pathways. *N. Engl. J. Med.* **360:** 44–52.
34. Perez-Tilve, D., S. M. Hofmann, J. Basford, R. Nogueiras, P. T. Pfluger, J. T. Patterson, E. Grant, H. E. Wilson-Perez, N. A. Granholm, M. Arnold, et al. 2010. Melanocortin signaling in the CNS directly regulates circulating cholesterol. *Nat. Neurosci.* **13:** 877–882.
35. Hildebrand, R. B., B. Lammers, I. Meurs, S. J. Korporaal, W. De Haan, Y. Zhao, J. K. Kruijt, D. Praticò, A. W. Schimmel, A. G. Holleboom, et al. 2010. Restoration of high-density lipoprotein levels by cholesteryl ester transfer protein expression in scavenger receptor class B type I (SR-BI) knockout mice does not normalize pathologies associated with SR-BI deficiency. *Arterioscler. Thromb. Vasc. Biol.* **30:** 1439–1445.